Temporal and spatial resolved optical emission behaviors of a cold atmospheric pressure plasma jet

Article *in* Journal of Applied Physics · November 2009

DOI: 10.1063/1.3239512 · Source: IEEE Xplore

13 authors, including:

Qing Xiong
Wuhan University
49 PUBLICATIONS **1,743** CITATIONS
SEE PROFILE

Xinpei Lu
Huazhong University of Science and Technology
170 PUBLICATIONS **6,465** CITATIONS
SEE PROFILE

Y. Xian
Huazhong University of Science and Technology
59 PUBLICATIONS **1,175** CITATIONS
SEE PROFILE

Zaiping Xiong
Institute of Applied Ecology,Chinese Academy of Sciences,Shenyang,China
42 PUBLICATIONS **1,050** CITATIONS
SEE PROFILE

Temporal and spatial resolved optical emission behaviors of a cold atmospheric pressure plasma jet

Q. Xiong, X. Lu,[a] J. Liu, Y. Xian, Z. Xiong, F. Zou, C. Zou, W. Gong, J. Hu, K. Chen, X. Pei, Z. Jiang, and Y. Pan
College of Electrical and Electronic Engineering, HuaZhong University of Science and Technology, WuHan, Hubei 430074, People's Republic of China

(Received 11 August 2009; accepted 4 September 2009; published online 22 October 2009)

The propagation behavior of cold atmospheric pressure plasma jets has recently attracted lots of attention. In this paper, a cold He plasma jet generated by a single plasma electrode jet device is studied. The spatial-temporal resolved optical emission spectroscopy measurements are presented. It is found that the emission intensity of the He 706.5 nm line of the plasma behaves similarly both inside the syringe and in the surrounding air (plasma plume). It decreases monotonously, which is different from the emission lines, such as N_2 337.1 nm line, N_2^+ 391.4 nm line, and O 777.3 nm line. For the discharge inside the syringe, the emission intensity of the He 706.5 nm line decays more rapidly than that of the other three spectral lines mentioned above. The N_2 337.1 nm line behaves a similar time evolution with the discharge current. For the N_2^+ 391.4 nm line and the atomic O 777.3 nm line, both of them decay slower than that of the He 706.5 nm and the N_2 337.1 nm. When the plasma plume propagates further away from the nozzle, the temporal behaviors of the emission intensities of the four lines tend to be similar gradually. Besides, it is found that, when the size of the plasma bullet appears biggest, the propagation velocity of the bullet achieves its highest value while the emission intensity of the N_2^+ 391.4 nm line reaches its maximum. Detailed analysis shows that the Penning effect between the metastable state He_m and the air molecules may play a significant role in the propagation of the plasma bullet in the open air. © *2009 American Institute of Physics*. [doi:10.1063/1.3239512]

I. INTRODUCTION

Cold atmospheric pressure plasma jets (C-APPJs) have recently attracted lots of attention because of their attractive characteristics.[1–12] C-APPJs can generate plasmas in open space rather than in confined discharge gaps, which make it possible for direct treatments, and have no limitation on the size of the objects to be treated. In addition, C-APPJs are normally under extreme nonequilibrium condition, where the electron temperature is much higher than the gas temperature. Their gas temperature can be as low as room temperature, which is very important for applications such as plasma medicine.[13–20]

Because of the potential applications mentioned above, various C-APPJ devices have been designed.[21–30] In order to improve the performance of the C-APPJs, detailed studies on the generation and propagation mechanisms of the plasma plumes are needed. High-speed photographs captured by intensified charge-coupled devices (ICCDs) revealed that some of the plasma plumes looks like continuously by bare eyes and are actually bulletlike plasma volumes with propagation speed of 10^4–10^5 m/s.[31–36] The bullet velocity is several orders of magnitude higher than that of the gas velocity. In addition, the propagation of the bullet is independent of the gas flow direction, which indicates that the plasma bullets are electrically driven.[31,33,35] Furthermore, studies show that the propagation behaviors of the plasma plumes are different from the positive streamer discharges, where the positive streamers are under high applied electric field. This is not the case for the plasma plume. The applied electric field along the plasma plume is much lower than that of the positive streamer discharges. Lu *et al.*[37] suggested that the propagation of the plasma plumes is attributed to the high local electric field induced by the head of the bullets. However, the mechanism of the propagation of the plasma plumes is still not well understood. To better understand the mechanism of the plasma bullet behavior, further studies, such as the spatial-temporal resolved emission behavior of the plasma plume, are needed.

The spatial-temporal resolved emission spectra from excited species, such as excited N_2, N_2^+, He, and O, may give us some inside information about the plasma bullet propagation mechanism. Besides, some of these excited species could be reactive, and they may play important roles in various applications.[24,38,39]

In this paper, the spatial-temporal resolved emission spectra of the plasma inside the syringe and in the surrounding air (plasma plume) are studied. It is found that the maximum propagation velocity of the plasma bullet is in correlation with the emission intensity of the 391.4 nm line of N_2^+. The rest of the paper is organized as follows. The experimental setup is described in Sec. II. Details of the experimental results, including the spatial-temporal resolved emission spectra inside and outside the syringe, and high-speed photographs of the plasma plume, are presented in Sec. III. Sec-

[a]Author to whom correspondence should be addressed. Electronic mail: luxinpei@hotmail.com.

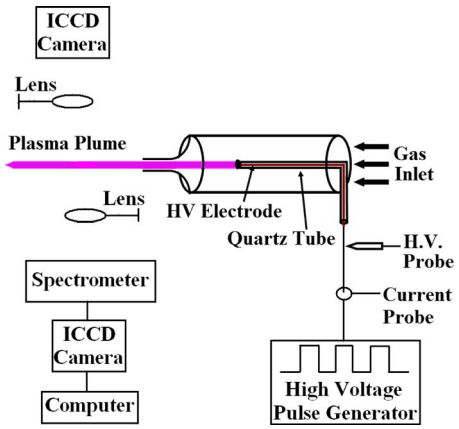

FIG. 1. (Color online) Schematic of the experimental setup.

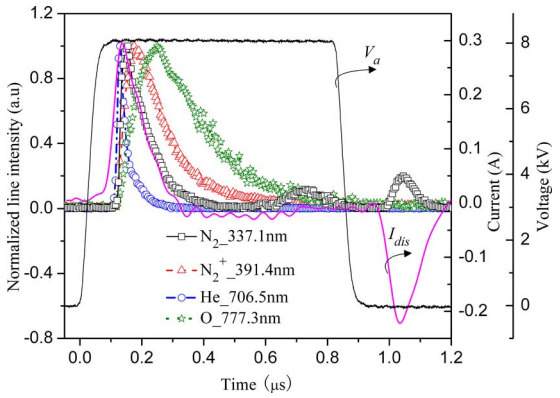

FIG. 2. (Color online) Temporal behavior of the normalized N_2 337.1 nm, N_2^+ 391.4 nm, He 706.5 nm, and O 777.3 nm intensities, discharge current I_{dis}, and applied voltage V_a. The emissions are from the plasma inside the syringe.

tion IV has a detailed discussion about the experimental results. Finally, Sec. V gives a brief summary of this work.

II. EXPERIMENTAL SETUP

Figure 1 shows the schematic of the experimental setup, which has been described in Ref. 14. Briefly, a high-voltage (HV) electrode made of a copper wire is inserted into a 10 cm long quartz tube with one end closed. The HV electrode together with the quartz tube is mounted inside another syringelike quartz tube. The distance between the closed end of the quartz tube and the nozzle is variable, which is fixed at 4 mm in this paper. Working gas such as He, Ar, or their mixtures with a small amount of air can be used. In this paper, He gas with a flow rate of 2 l/min is used.

The device is driven by a pulsed dc power supply with amplitudes up to 10 kV, repetition rate up to 10 kHz, and pulse width variable from 200 ns to dc. The applied voltage is measured by a P6015 Tektronix HV probe and the current by a Tektronix TCP202 current probe. The voltage and current waveforms are recorded by a Tektronix DPO7104 digital oscilloscope.

The spatial-temporal resolved optical emission spectra are measured by a half meter spectrometer (Princeton Instruments Acton SpectraHub 2500i) and detected by an ICCD camera (Princeton Instruments, Model PIMAX2). The ICCD camera is also used to capture the dynamics of the plasma plume. For both the spectra measurements and the fast imaging, the exposure time of the ICCD camera is set at 5 ns.

III. EXPERIMENTAL RESULTS

For all the measurements, the applied voltage V_a, pulse width t_{pw}, and pulse repetition rate f are fixed at 8 kV, 800 ns, and 4 kHz, respectively.

When He gas with a flow rate of 2 l/min is introduced into the syringe and HV is applied to the HV electrode, a homogeneous discharge is ignited inside the syringe and a He plasma plume is generated in the open air. Because of the air diffusion, the emission spectrum of the plasma inside the syringe and the plasma plume in the surrounding air are similar to the traditional dielectric barrier discharge He mixed with a small amount of air.[40–42] In addition to the atomic He lines, the N_2 and N_2^+ ion rotational bands, and the atomic O lines are also observed. The emission intensity of a spectral line is directly related to the population of the excited state particle at the upper level of the transition that emits the line. The emission intensity of a spectral line is also related to the collisional quenching effect and the electron temperature. The collisional quenching has a negative effect on the population of the upper level. For example, the emission intensity of the He 706.5 nm line decreases dramatically when 1% of air is added in the He gas discharge. This is partly due to the reduction in the upper level He($3\ ^3S_1$) by the air molecules through the collisional quenching effect. In general, a higher average electron temperature can lead to an increase in the population of the excited particle at a high-energy level and induce an increase in the emission intensity of the corresponding spectral line. However, this is not the case when the electron temperature is too high and adverse for the electron collision cross section. In this paper, we focus on four spectral lines, i.e., N_2 ($C\ ^3\Pi_u$, $\nu_C=0 \rightarrow B\ ^3\Pi_g$, $\nu_B=0$) at 337.1 nm, N_2^+ ($B\ ^2\Sigma_u^+$, $\nu_B=0 \rightarrow X\ ^2\Sigma_g^+$, $\nu_X=0$) at 391.4 nm, He($3\ ^3S_1 \rightarrow 2\ ^3P_{0,1,2}$) at 706.5 nm, and O($3p\ ^5P \rightarrow 3s\ ^5S$) at 777.3 nm. The spatial-temporal resolved emission intensities of the selected lines from the plasma inside and outside the syringe are studied.

Figure 2 shows the temporal emission behavior of the four spectral lines inside the syringe and the current-voltage (I-V) waveforms of the discharge. In order to obtain a better comparison of the temporal emission behaviors and the I-V waveforms, the four emission lines are normalized. It should be pointed out that the discharge current I_{dis} is the actual discharge current with a peak value of about 300 mA, which is obtained by subtracting the displacement current from the total current.[14] As shown in Fig. 2, immediately after the breakdown, the emission intensity of the four spectral lines increases. The current increases to its peak value after the applied voltage reached its plateau value. At the same moment, the He 706.5 nm line reaches its maximum emission intensity too. Then, the current and the He 706.5 nm line begin to decrease. As can be seen, the He 706.5 nm line decreases much faster than that of the current. The N_2 337.1 nm line has a similar behavior as the discharge current. Regarding the N_2^+ 391.4 nm line and the atomic O 777.3 nm

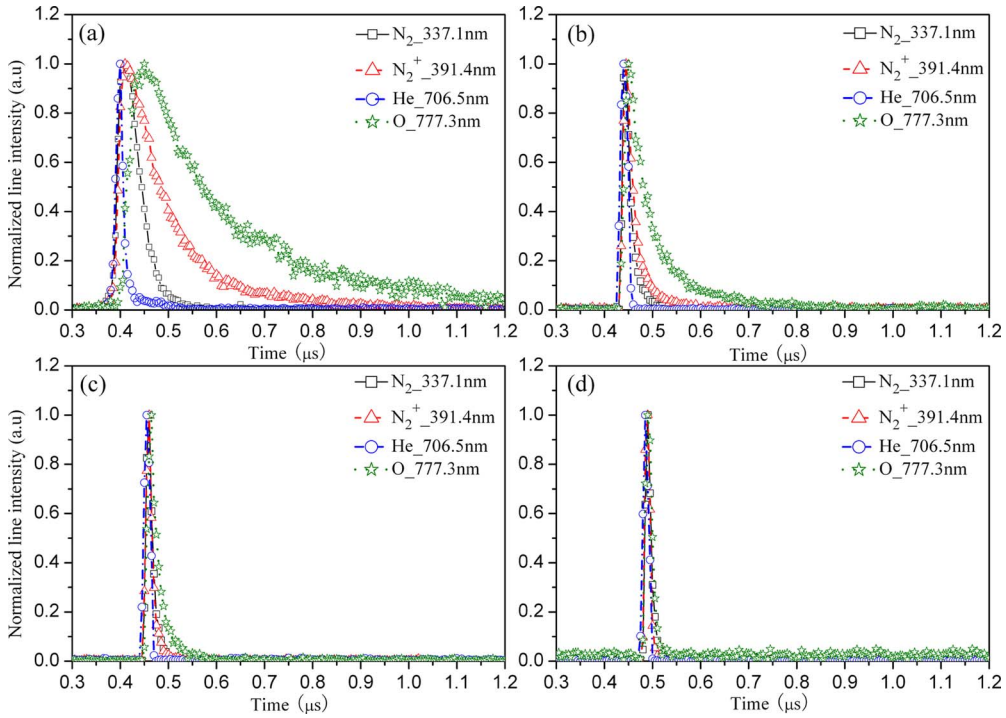

FIG. 3. (Color online) Temporal behavior of the normalized N_2 337.1 nm, N_2^+ 391.4 nm, He 706.5 nm, and O 777.3 nm lines at various positions: (a) 3, (b) 8, (c) 13, and (d) 18 mm along the He plasma plume in the open air.

line, both of them rise and decay slower than that of the current. More discussion on these observations will be given in Sec. IV. After the arrival of the falling front of the applied voltage, a negative current pulse starts at about 0.95 μs. The negative current is related to a second breakdown, which is induced by the charges accumulated on the inner surface of the syringe. Immediately after that, a N_2 emission can be observed. This N_2 emission pulse is similar as the time evolution of the current, and both reach their peak values at almost the same moment. Except the N_2 337.1 nm emission line, the optical emissions of the other three lines are not observed during this period.

In order to have a better understanding of the propagation mechanism of the He plasma plume in the open air, the spatial-temporal resolved optical emission spectroscopy (OES) measurements are carried out onto the plume. Figures 3(a)–3(d) show the time evolution of the normalized emission intensities of the four spectral lines at various positions along the plasma plume. At 3 mm away from the nozzle, as shown in Fig. 3(a), the temporal behaviors of the emission intensities of the four lines are similar to that of the positive discharge inside the syringe. The He 706.5 nm line decays much faster than the other three lines. However, it should be pointed out that the time difference of the four lines reaching their peak intensity is smaller than that inside the syringe. This trend becomes more obvious as the plume propagates further in the open air. As shown in Fig. 3(b), the four spectral lines reached their peak values almost simultaneously for the plume of 8 mm away from the nozzle. Besides, the N_2 337.1 nm, the N_2^+ 391.4 nm and the O 777.3 nm from the plasma plume far away from the nozzle decay faster than that close to the nozzle. As shown in Figs. 3(c) and 3(d), they decay even faster when the plasma plume propagates further far away from the nozzle. At 18 mm away from the nozzle, all the four lines decay simultaneously.

Figure 4 shows the spatially resolved normalized emission intensities of the four spectral lines along with the propagation velocity of the plasma bullet. As can be seen, the He 706.5 nm decays as soon as the plasma plume propagates in the open air. However, the N_2^+ 391.4 nm and O 777.3 nm line intensities increase dramatically in the beginning when the plume propagates out of the nozzle. The two lines reach their maxima at about 8 mm away from the nozzle. It is interesting to point out that the bullet velocity reaches its maximum value of 2.1×10^5 m/s at almost the same position. The N_2 337.1 nm line increases slowly and reaches its maximum at about 20 mm away from the nozzle. Figure 5 shows the high-speed photographs of the plasma bullet

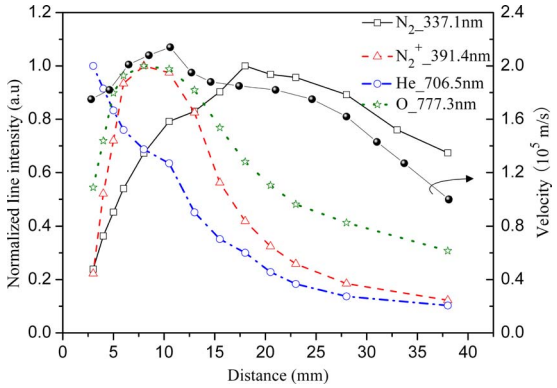

FIG. 4. (Color online) Spatial distribution of the normalized N_2 337.1 nm, N_2^+ 391.4 nm, He 706.5 nm, and O 777.3 nm intensities, and the bullet velocity along the He plasma plume in the open air.

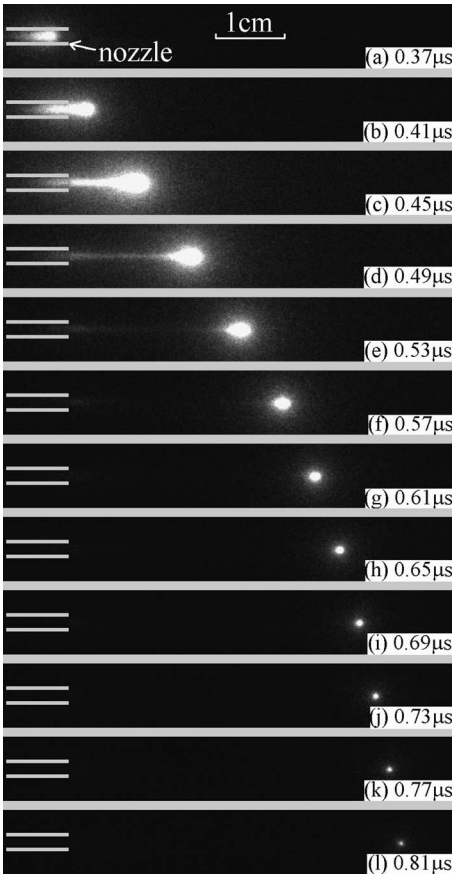

FIG. 5. High-speed photographs of the He plasma plume in the open air with exposure time fixed at 5 ns. Photographs (a)–(l) are taken at 40 ns increments.

propagating in the open air. The time delay marked in Fig. 5 corresponds to that shown in Fig. 2. Based on Figs. 4 and 5, it is noteworthy that the size of the bullet appears biggest while the velocity of bullet achieves its highest value and the emission intensity of the N_2^+ 391.4 nm line reaches its maximum too. More discussion on this observation will also be given in Sec. IV.

IV. DISCUSSION

In pure He gas discharge, the quenching of the excited state He($3\ ^3S_1$) is mainly due to the collisions with the ground state He atoms.[43] In our experiment, because of the air diffusion, the quenching mechanism of the He($3\ ^3S_1$) (including the metastable state He_m) is Penning effect with air molecules. Due to quenching, the effective lifetime of the He($3\ ^3S_1$) decreases when air diffuses into the discharge. Especially plasma plume in the open air, where the air percentage is much higher than that inside the syringe, the effective lifetime of the He($3\ ^3S_1$) is shorter. This can lead to a decrease in the emission intensity of the He 706.5 nm line. With regard to the other three excited species, i.e., $N_2(C\ ^3\Pi_u,\ \nu_C=0)$, $N_2^+(B\ ^2\Sigma_u^+,\ \nu_B=0)$, and $O(3p\ ^5P)$, their effective lifetimes will also decrease due to the collisional quenching when the air percentage increases. For example, the effective lifetime of the $N_2^+(B\ ^2\Sigma_u^+,\ \nu_B=0)$ decreases to only about 5 ns when the nitrogen partial pressure is 2 kPa.[44] The radiative lifetimes of the three excited species mentioned above are 40, 66, and 34 ns, respectively.[44–46] When the effective lifetime decreases smaller than the radiative lifetime, the collisional quenching can play an adverse effect on the emission intensity. However, it is not the case for the discharge inside the syringe, where the air percentage is small (<1%). It may have a negative effect on the emission intensity of the plasma plume in the open air.

A. Plasma inside the syringe

1. Temporal behavior of the He emission

The emission intensity of a spectral line is directly related to the population of the excited state at the upper level of the transition emitting the line. The spectral line 706.5 nm is ascribed to the transition ($3\ ^3S_1 \rightarrow 2\ ^3P_{0,1,2}$) of excited He atoms. The excited state He($3\ ^3S_1$) can be produced through several processes, including direct excitation collisions by high-energy electrons with ground state He atoms, cascade transitions from upper levels, step-excitation collisions between excited state He atoms at lower excited levels (such as metastable states), and low-energy electrons. Because of the absence of the emission spectrum corresponding to the transitions from upper levels to $3\ ^3S_1$, the effect of cascade transitions on the generation of He($3\ ^3S_1$) is very small and negligible. And the step excitations from the metastable states, He($2\ ^1S$) and He($2\ ^3S$), are also very small because the *S*-*S* transitions are forbidden. Therefore, the He($3\ ^3S_1$) during the positive discharge is mainly produced by the high-energy electrons through electron collisions with ground state He atoms. The high-energy electrons can be produced during the fast rise phase of the HV pulses, which results in the generation of the excited state He($3\ ^3S_1$) through direct collisions with electrons and emits the He 706.5 nm line. The He emission intensity increases to its maximum while the discharge current reaches its peak. Then, because the electric field induced by the charges deposited on the surface of the dielectric, the electric field decreases dramatically, which may result in the decrease in the electron temperature. In other words, much less high-energy electrons are generated in the plasma. Thus, the rapid decay of the He emission intensity may indicate a fast decrease in the electron temperature.[47]

2. Temporal behavior of the N_2 emission

The emission at 337.1 nm is from the transition ($C\ ^3\Pi_u,\ \nu_C=0 \rightarrow B\ ^3\Pi_g,\ \nu_B=0$) of N_2. The state $N_2(C\ ^3\Pi_u,\ \nu_C=0)$ can be populated by a number of processes including through direct electron collisions with the ground state nitrogen molecules N_2 (threshold level $E_{\text{threshold}}=11$ eV), the step excitation from excited states $N_2(A\ ^3\Sigma_u^+)$ and $N_2(B\ ^3\Pi_g)$. As can be seen, the emission intensity of the N_2 337.1 nm line rises almost synchronously with the discharge current. During this rising phase, the state $N_2(C\ ^3\Pi_u,\ \nu_C=0)$ is probably mainly generated through the direct electron collision excitation. This may be explained by the following two reasons. First, the generation of the He emission mentioned above suggests the presence of the high-energy electrons during the current rising phase. The high-energy electrons can easily transfer energy to the ground state N_2 and generate $N_2(C\ ^3\Pi_u,\ \nu_C=0)$. Second, the step-

excitation process is based on the generation of $N_2(A\ ^3\Sigma_u^+)$ and $N_2(B\ ^3\Pi_g)$. Then $N_2(C\ ^3\Pi_u,\ \nu_C=0)$ is generated through the collisions between electrons and $N_2(A\ ^3\Sigma_u^+)$ and $N_2(B\ ^3\Pi_g)$. If this process is dominant, it will result in a time delay between the N_2 emission and the discharge current during the rising phase. But this time decay is not observed in our experiment. On the other hand, this step-excitation process probably plays an important role in the decay phase of the N_2 emission. As can be seen, the N_2 emission decreases slower than that of the He. During the decay phase, the population of the high-energy electrons decreased rapidly. The generation of the $N_2(C\ ^3\Pi_u,\ \nu_C=0)$ during this phase may be mainly through the collisions between the low-energy electrons and the excited states $N_2(A\ ^3\Sigma_u^+)$ and $N_2(B\ ^3\Pi_g)$.

3. Temporal behavior of the N_2^+ emission

The emission at 391.4 nm is ascribed to the transition $(B\ ^2\Sigma_u^+,\ \nu_B=0 \rightarrow X\ ^2\Sigma_g^+,\ \nu_X=0)$ of ions N_2^+. During the rising phase of the N_2^+ 391.4 nm line, the generation of the state $N_2^+(B\ ^2\Sigma_u^+,\ \nu_B=0)$ is mainly through the direct electron collisions with the high-energy electrons. However, this process is not the case during the decay phase. As can be seen, the emission intensity of the N_2^+ 391.4 nm line decays much slower than that of the discharge current. During the decay phase, the generation of the state $N_2^+(B\ ^2\Sigma_u^+,\ \nu_B=0)$ may be related to other two important reactions as follows.[48]

For charge transfer reaction,

$$He_2^+ + N_2 \rightarrow 2He + N_2^+(B\ ^2\Sigma_u^+),$$

$$k_1 = 5 \times 10^{-10}\ \text{cm}^3\ \text{s}^{-1}. \quad (1)$$

For Penning ionization,

$$He_m + N_2 \rightarrow He + N_2^+(B\ ^2\Sigma_u^+) + e,$$

$$k_2 = 7 \times 10^{-11}\ \text{cm}^3\ \text{s}^{-1}. \quad (2)$$

The long-living metastable state He_m can lead to a long decay phase of the population of the state $N_2^+(B\ ^2\Sigma_u^+,\ \nu_B=0)$, which results in a slow decrease in N_2^+ emission. With regard to charge transfer reaction (1), it may be not important during the decay phase because the positive ions are normally dominant by N_2^+ or N_4^+ but not He_2^+ in the plasma with He mixed with a small amount of nitrogen molecules.[49]

4. Temporal behavior of the O emission

The spectral line O 777.3 nm is from the transition $(3p\ ^5P \rightarrow 3s\ ^5S)$ of oxygen atom O. The generation of the state $O(3p\ ^5P)$ at the early phase of the positive discharge can be partly ascribed to the direct electron-molecule dissociative collisions between the high-energy electrons and the ground state O_2 $(E_{\text{threshold}}=15.87\ \text{eV})$. However, the O 777.3 nm line reached its maximum emission intensity at about 0.25 μs, while the discharge current has decreased dramatically. So the excited O is not mainly generated by collisions with electrons. One of the generation processes is related to the following Penning reaction with the metastable state He_m:

$$He_m + O_2 \rightarrow He + O(3p\ ^5P) + O. \quad (3)$$

During the decay phase, the decrease in the state $O(3p\ ^5P)$ is mainly ascribed to the recombination with O_2 to form O_3. This reaction process is relatively slow. That is the reason why the O emission intensity decays much slower.

B. He plasma plume in the open air

As can be seen, the emission intensity of the He 706.5 nm line decreases as the plasma plume propagates in the open air. This is ascribed to the diffusion of the ambient air into the He plasma plume. The energy of the electrons in the plasma can be lost through frequent collisions with N_2 and O_2. Because of the low threshold energy, the molecular gases can obtain energy from the electrons to be excited to their rotational states and vibrational states. In addition, the low dissociation energy of the molecular gases, such as O_2, NO, and NO_2, may also play a role in the energy loss of electrons. And because of low electron affinity energy of the electronegative O_2 molecules (about 0.45 eV), the electrons are more easily lost in the formation of the O_2^- ions. This also can be adverse to the increase in the energy of electrons. Because the external electric field along the plasma plume is low, the population of the high-energy electrons in the plume will further decrease due to the air diffusion. That is why the He emission intensity becomes much lower than that of the plasma inside the syringe. As the plume propagates further in the open air, the air percentage in the plume keeps increasing, which results in much less high-energy electrons and so weak He emission. However, except the He 706.5 nm line, the emission intensities of the other three lines increase as soon as the plume comes out of the nozzle. With regard to the N_2^+ 391.4 nm and the O 777.3 nm, at the position next to the nozzle, the air percentage is probably too low. With the propagation of the plume, the air percentage increases, which results in an enhanced Penning effect. After they reach their maxima, the decrease in He_m population plays a dominant role in the process. Accordingly, the N_2^+ and O emission intensities start to decrease as the plume propagates further. With regard to the emission intensity of the N_2 337.1 nm line, which reaches its peak at about 20 mm away from the nozzle, this may be explained as follows. The threshold energy of the state $N_2(C\ ^3\Pi_u,\ \nu_C=0)$ is much lower than that of the $N_2^+(B\ ^2\Sigma_u^+,\ \nu_B=0)$ and $O(3p\ ^5P)$. So $N_2(C\ ^3\Pi_u,\ \nu_C=0)$ can still be generated through various processes such as step excitation. And the pooling reaction of the excited state $N_2(A)$ may also play a role in the generation of the $N_2(C\ ^3\Pi_u,\ \nu_C=0)$.[50,51]

As reported previously, the plasma bullet travels in high speed, which is qualitatively equivalent to the electron drift velocity v_e.[31,35] This high bullet velocity v_b can be characterized by the electron drift velocity v_e. On the other side, the propagation of the plasma plume is attributed to the high local electric field E_{loc} induced by the head of the bullets.[37] The electron drift velocity v_e is dominated by the local electric field E_{loc}. Therefore, the high bullet velocity v_b is also directly related to the local electric field E_{loc}. Furthermore, the local electric field E_{loc} is proportional to the charges Q carried by the bullet. When the N_2^+ emission intensity in-

creases, indicating more nitrogen molecules are ionized, a larger amount of charges are generated in the bullet. Thus stronger local electric field is induced in front of the bullet. Electrons travel toward the bullet head much more quickly, which results in a high bullet velocity. This is consistent with our experimental observations.

V. CONCLUSION

In summary, the spatial-temporal resolved emission behaviors of the plasma inside the syringe and the He plasma plume in the open air are investigated. Inside the syringe, the emission intensity of the He 706.5 nm line decays more rapidly than that of the other three spectral lines. The N_2 337.1 nm line behaves a similar time evolution with the discharge current. The N_2^+ 391.4 nm and O 777.3 nm both decay relatively slowly. Besides, the emission intensities of all the lines for the negative discharge are much weaker than that of the positive discharge. During the negative discharge, only the emission of the N_2 lines are observed. When the plasma propagates out of the syringe nozzle, the diffusion of the ambient air has a significant effect on the propagation of the plasma plume in the open space, which reduces the population of the high-energy electrons and He_m metastable states. As a result, the emission intensity of the He 706.5 nm line is much weaker than that inside the syringe. Except the He 706.5 nm line, the other three lines all start to decay rapidly as the plasma plume propagates in the open air. And it is found that the emission intensities of the three lines, N_2 337.1 nm, N_2^+ 391.4 nm, and O 777.3 nm, all increase first and then decrease as the propagation of the plume in the open air, which is different with the monotonous decrease in the He 706.5 nm line. Besides, the Penning effect induced by the metastable state He_m with N_2/O_2 plays a crucial role in the dynamics of the plasma bullet in the open air. The plasma bullet velocity reaches its maximum while the emission intensity of the N_2^+ 391.4 nm line reaches its peak.

ACKNOWLEDGMENTS

This work was supported in part by the National Natural Science Foundation under Grant No. 10875048, and in part by the Chang Jiang Scholars Program, Ministry of Education, People's Republic of China.

[1]M. Laroussi and T. Akan, Plasma Processes Polym. **4**, 777 (2007).
[2]J. Walsh and M. Kong, Appl. Phys. Lett. **91**, 221502 (2007).
[3]R. Dorai and M. Kushner, J. Phys. D **36**, 666 (2003).
[4]G. Fridman, G. Friedman, A. Gutsol, A. Shekhter, V. Vasilets, and A. Fridman, Plasma Processes Polym. **5**, 503 (2008).
[5]Q. Nie, C. Ren, D. Wang, and J. Zhang, Appl. Phys. Lett. **93**, 011503 (2008).
[6]I. Kieft, D. Darios, A. Roks, and E. Stoffels, IEEE Trans. Plasma Sci. **33**, 771 (2005).
[7]M. Laroussi and X. Lu, Appl. Phys. Lett. **87**, 113902 (2005).
[8]X. Lu, Z. Jiang, Q. Xiong, Z. Tang, X. Hu, and Y. Pan, Appl. Phys. Lett. **92**, 081502 (2008).
[9]S. Li, W. Huang, J. Zhang, and D. Wang, Phys. Plasmas **16**, 073503 (2009).
[10]Z. Cao, J. Walsh, and M. Kong, Appl. Phys. Lett. **94**, 021501 (2009).
[11]Q. Xiong, X. Lu, K. Ostrikov, Z. Xiong, Y. Xian, F. Zhou, C. Zou, J. Hu, W. Gong, and Z. Jiang, Phys. Plasmas **16**, 043505 (2009).
[12]D. Mariotti, Appl. Phys. Lett. **92**, 151505 (2008).
[13]A. Shashurin, M. Keidar, S. Bronnikov, R. Jurjus, and M. Strpp, Appl. Phys. Lett. **93**, 181501 (2008).
[14]X. Lu, Z. Jiang, Q. Xiong, Z. Tang, and Y. Pan, Appl. Phys. Lett. **92**, 151504 (2008).
[15]Y. Hong and H. Uhm, Phys. Plasmas **14**, 053503 (2007).
[16]F. Iza, G. Kim, S. Lee, J. K. Lee, J. Walsh, Y. Zhang, and M. Kong, Plasma Processes Polym. **5**, 322 (2008).
[17]G. Li, H. Li, L. Wang, S. Wang, H. Zhao, W. Sun, X. Xing, and C. Bao, Appl. Phys. Lett. **92**, 221504 (2008).
[18]G. Fridman, A. Brooks, M. Galasubramanian, A. Fridman, A. Gutsol, V. Vasilets, H. Ayan, and G. Friedman, Plasma Processes Polym. **4**, 370 (2007).
[19]J. Goree, B. Liu, and D. Drake, J. Phys. D **39**, 3479 (2006).
[20]J. Lim, H. Uhm, and S. Li, Phys. Plasmas **14**, 093504 (2007).
[21]Y. Hong and H. Uhm, Appl. Phys. Lett. **89**, 221504 (2006).
[22]K. Becker, K. Schoenbach, and J. Eden, J. Phys. D **39**, R55 (2006).
[23]X. Zhang, J. Huang, X. Liu, L. Peng, L. Guo, G. Lv, W. Chen, K. Feng, and S. Yang, J. Appl. Phys. **105**, 063302 (2009).
[24]X. Lu, T. Ye, Y. Cao, Z. Sun, Q. Xiong, Z. Tang, Z. Xiong, J. Hu, Z. Jiang, and Y. Pan, J. Appl. Phys. **104**, 053309 (2008).
[25]X. Lu, Y. Cao, P. Yang, Q. Xiong, Z. Xiong, Y. Xian, and Y. Pan, IEEE Trans. Plasma Sci. **37**, 668 (2009).
[26]T. Ni, F. Ding, X. Zhu, X. Wen, and H. Zhou, Appl. Phys. Lett. **92**, 241503 (2008).
[27]J. Kolb, A. Mohamed, R. Price, R. Swanson, A. Bowman, R. Chiavarini, M. Stacey, and K. Schoenbach, Appl. Phys. Lett. **92**, 241501 (2008).
[28]E. Stoffels, I. Kieft, and R. Sladek, J. Phys. D **36**, 2908 (2003).
[29]J. Walsh and M. Kong, Appl. Phys. Lett. **93**, 111501 (2008).
[30]D. Kim, J. Rhee, B. Gweon, S. Moon, and W. Choe, Appl. Phys. Lett. **91**, 151502 (2007).
[31]X. Lu and M. Laroussi, J. Appl. Phys. **100**, 063302 (2006).
[32]A. Shashurin, M. Shneider, A. Dogariu, R. Miles, and M. Keidar, Appl. Phys. Lett. **94**, 231504 (2009).
[33]M. Teschke, J. Kedzierski, E. Finantu-Dinu, K. Korzec, and J. Engemann, IEEE Trans. Plasma Sci. **33**, 310 (2005).
[34]B. Sands, B. Ganguly, and K. Tachibana, Appl. Phys. Lett. **92**, 151503 (2008).
[35]R. Ye and W. Zheng, Appl. Phys. Lett. **93**, 071502 (2008).
[36]N. Mericam-Bourdet, M. Laroussi, A. Begum, and E. Karakas, J. Phys. D **42**, 055207 (2009).
[37]X. Lu, Q. Xiong, Z. Xiong, J. Hu, F. Zhou, W. Gong, Y. Xian, C. Zhou, Z. Tang, Z. Jiang, and Y. Pan, J. Appl. Phys. **105**, 043304 (2009).
[38]E. Stoffels, Y. Sakiyama, and D. Graves, IEEE Trans. Plasma Sci. **36**, 1441 (2008).
[39]M. Laroussi, Plasma Processes Polym. **2**, 391 (2005).
[40]G. Nersisyan and W. Graham, Plasma Sources Sci. Technol. **13**, 582 (2004).
[41]F. Massines, P. Segur, N. Gherardi, C. Khamphan, and A. Ricard, Surf. Coat. Technol. **174–175**, 8 (2003).
[42]A. Ricard, P. Decomps, and F. Massines, Surf. Coat. Technol. **112**, 1 (1999).
[43]R. Deloche, P. Monchicourt, M. Cheret, and F. Lambert, Phys. Rev. A **13**, 1140 (1976).
[44]N. Bibinov, A. Fateev, and K. Wiesemann, Plasma Sources Sci. Technol. **10**, 579 (2001).
[45]G. Cartry, L. Magne, and G. Cernogora, J. Phys. D **32**, 1894 (1999).
[46]E. Collart, J. Baggerman, and R. Visser, J. Appl. Phys. **70**, 5278 (1991).
[47]X. Lu and M. Laroussi, Appl. Phys. Lett. **92**, 051501 (2008).
[48]X. Yuan and L. Raja, IEEE Trans. Plasma Sci. **31**, 495 (2003).
[49]T. Martens, A. Bogaerts, W. Brok, and J. Dijk, Appl. Phys. Lett. **92**, 041504 (2008).
[50]P. Bruggeman, D. Schram, M. Gonzalez, R. Rego, M. Kong, and C. Leys, Plasma Sources Sci. Technol. **18**, 025017 (2009).
[51]N. Bibinov, A. Fateev, and K. Wiesemnn, J. Phys. D **34**, 1819 (2001).